ISSN 2347 - 3983
Volume 7, No. 9 September 2019
International Journal of Emerging Trends in Engineering Research
Available Online at http://www.warse.org/IJETER/static/pdf/file/ijeter06792019.pdf
https://doi.org/10.30534/ijeter/2019/06792019

Characterization of (CMC-PVP- Fe_2O_3) Nanocomposites for Gamma Shielding Application

Majeed Ali Habeeb , Waleed Shaker Mahdi
University of Babylon, College of Education for Pure Sciences , Department of Physics , Iraq
majeed_ali74@yahoo.com

ABSTRACT

The [(CMC)– (PVP) – Fe_2O_3] nanocomposites were prepared by using casting method with different percentages (0,1.5,3,4.5,6)wt% of Fe_2O_3. Optical microscope images show the iron oxides from a continuous network inside the polymers when the proportion of(6 wt%). FTIR spectra shows shift in peak position as well as the change in shape and intensity. The absorbance and absorption coefficient of (CMC– PVP – Fe_2O_3) nanocomposites increased with increasing of the iron oxide nanoparticles. Transmittance decrease with increasing of the iron oxide nanoparticles. The optical energy gap decreases with increasing of Fe_2O_3 nanoparticles and the extinction coefficient increases with increase of Fe_2O_3 nanoparticles. The real and imaginary dielectric constant is increased with increase of Fe_2O_3 .The optical conductivity of nanocomposites is increased with increase of Fe_2O_3 nanoparticles. The transmission radiation decreases with the increasing of the concentrations of Fe_2O_3. The attenuation coefficients increase with increased of concentration.

Key words: Nanocomposites , structural , optical properties , gamma ray shielding

1. INTRODUCTION

Nanoparticles are the easiest type of 1-100nm size constructions. Iron oxide nanoparticles were synthesized by cost effective co-precipitation method. It possesses strong ferromagnetic behavior and less sensitivity to oxidation. Iron oxide nanoparticles have attracted much interest because they belong to the class of materials having non-toxicity and biological compatibility due to the presence of Fe ions[1]. PVP deserve a special attention among the conjugated polymers because of its good environmental stability, easy processability, moderate electrical conductivity and rich physics in charge transport mechanism. It is an amorphous polymer and possesses high glass transition temperature (Tg) values up to 100 °C because of the presence of the rigid pyrrolidone group. In solution, it has excellent wetting properties and readily forms films. This makes it good as a coating or an additive to coatings. It is commonly used in medicine because of its extremely low cytotoxicity. Its other applications can be found in controlled drugrelease technology and electrochemical devices (batteries, displays) [2]. Carboxyl methyl Cellulose (CMC) is a natural biodegradable and biocompatible anionic polymer receiving from natural cellulose by chemical modification. Moreover, CMC could be used as potential fat replacers where it is non-digestible fibers [3]. Carboxymethyl cellulose may be coatings only and in blend with gamma irradiation was experienced for keeping the storage quality and improving shelf-life of plum. CMC-based coatings can be shared with gamma irradiation to achieve a synergistic influence concerning to storage quality and shelf-life of fresh fruits [4]. CMC is used for keeping moisture, and enhancing the mouth-feel and structural consistency of bakery products; it is also used in blending with other stabilizers and gums because of its high water absorbing capacity [5].There are some basic principles for radiation shielding depending on distance and time. The type and amount of shielding required depend on the type of radiation, the activity of the radiation source and the dose rate. However, there are other factors for the choice of shielding material such as their cost and weight. An effective shield will result in a large energy loss in a small penetration distance without emission of radiation [6].

2 .EXPERIMENTAL PROCEDURE

The (CMC-PVP- Fe_2O_3) nanocomposites films were prepared by using casting method with different concentrations are (0 , 1.5 , 3 , 4.5 and 6) wt%. The optical properties of nanocomposites films were measured by using the double beam spectrophotometer (shimadzu, UV-1800°A) in wavelength (220–800) nm. The optical microscope , which is supplied from Olympus name (Toup View) type (Nikon – 73346) .FTIR spectrum were recorded by FTIR (Bruker company , German origin , type vertex -70) fourier transform infrared spectrometer in the wave number range (400 – 4000)cm^{-1} .

3.RESULTS AND DISCUSSION

3.1.The Optical Microscope

Figure 1 shows the images of (CMC-PVP- Fe_2O_3) nanocomposites films, taken for samples of different concentrations at magnification power 10x. However, they show a clear difference to the samples as shown in Figure 2 (A,B,C,D and E). When increasing proportions of iron oxide nanoparticles in films (Carboxy Methyl Cellulos – Poly (VinylePyrrolidone)), when the concentration reaches to 6

wt.% for (CMC-PVP- Fe_2O_3) nanocomposites, the nanoparticles form a continuous network inside the polymers. This network has paths where charge carriers are allowed to pass through the paths, causing a change in the material properties [7,8,9].

3.2. Fourier Transform Infrared Radiation (FTIR)

FTIR has been used to analyze the interactions among atoms or ions in (CMC-PVP-Fe_2O_3) nanocomposites. These interactions can include changes in the vibrational modes of the nanocomposites. The (FTIR) transmittance spectra of (CMC-PVP-Fe_2O_3) nanocomposites films with the different ratio of Fe_2O_3 nanoparticles are shown in Figure 2 (A, B, C, D and E), recorded at room temperature in the range (600–4500) cm^{-1}. From the infrared spectra, it can be noticed that the variation of (Fe_2O_3) nanoparticles ratio causes some observable changes in the spectrum of (CMC-PVP). It induces some new absorption bands and slight changes in the intensities of some absorption bands. The new absorption bands may be correlated, likewise to defects induced by the charge-transfer reaction between the polymers chain and the dopant. From the spectra, the FTIR spectrum of (CMC-PVP) film shows broad and strong bands are observed at 3750 cm^{-1} which is assigned to O–H stretching vibration of hydroxyl groups and 2921 cm^{-1} is assigned to C–H stretching vibration. The peaks at 1558 and 1457 cm^{-1} have been attributed to the C=O, C=C stretching mode. The strong band at 1772-1457 cm^{-1} has been attributed to the stretching mode of C-H and C-O groups. The band at about 1019 cm^{-1} corresponds to C–O ,While the absorption band at about 618 cm^{-1} is assigned to out of plane rings C–H bending. The band relating to the pyrrolidone C= O group is located at 1698 cm^{-1}. The bands at 618 cm^{-1}, 1019 cm^{-1} and 1457 cm^{-1} are attributed to C–C stretching vibratio, C–N stretching vibration and C–H bending vibration of pure respectively . In case of (CMC-PVP-Fe_2O_3) is with different (Fe_2O_3) ratio. FTIR spectra shows shift in peak position as well as the change in shape and intensity, comparing with pure (CMC-PVP) composites, this indicates decoupling between the corresponding vibration of two polymer and iron oxide[10]

3.3 The Optical Properties.

3.3.1 Absorbance

Figure 3 demonstrates the absorption spectrum of nanocomposites (CMC-PVP-Fe_2O_3) as a function of the wavelength of the incident light. We can be noticed from the figure that absorption for all films have a high values at wavelength in the neighborhood of the fundamental absorption edge (250 nm) , then the absorbance decreases with the increasing of wavelength. In general, the absorbance of films is increased in the ultraviolet region and decreases in visible area and infrared area due to high wavelength. The incident photon doesn't have enough energy to interact with atoms, thus the photon will be transmitted. When the wavelength decreases, the interaction between incident photon and material will occur, and the photon will absorbance, and then the absorbance will increase [10].Consequently ,by the increase of the weight percentages of iron oxide nanoparticles , absorbance is increased .These results are similar to the results reached by the researchers [11].

3.3.2 Transmittance

Figure 4 demonstrates the optical transmittance spectrum by incorporating distinct rates of (Fe_2O_3) nanoparticles as a function of incident light wavelength on (CMC-PVP- Fe_2O_3) movies .This figure shows that transmittance decrease with the increase of the added Fe_2O_3 concentration, this is caused by Fe2O3 electrons in its outer orbits which can absorb the electromagnetic energy of the incident light and travel to higher energy levels. This process is not accompanied by emission of radiation because the traveled electron to higher levels occupied vacant positions of energy bands, thus part of the incident light is absorbed by the substance and dose not penetrate through it ,on the other hand, the pure poly(vinyl pyrrolidone) has high transmittance because there is no free electron (i.e. electrons are linked to atoms by covalent bonds) ,this is because the breaking of electron linkage and moving it to the conduction band need to photon with high energy [12].

3.3.3 Absorption Coefficient

Figure 5 shows the absorption coefficient $\alpha(cm)^{-1}$ as a function of photon energy for (CMC-PVP- Fe_2O_3) nanocomposites .We can see that the absorption coefficient is increased with the increase of the concentrations of Fe_2O_3 nanoparticles. The reason is due to the increase of the number of charge carriers, hence, increase the absorbance of (CMC-PVP- Fe_2O_3) and absorption coefficient [13,14].

3.3.4 Optical Energy Gaps of the (Allowed and Forbidden) Indirect Transition

Figure 6 shows the relation between absorption edge $(\alpha h\upsilon)^{1/2}$ for (CMC-PVP- Fe_2O_3) nanocomposites as a function of photon energy .We can see that the values of energy gap decrease with increasing the Fe_2O_3 nanoparticles concentrations,this is attributed to the increase of disorder in the material, that means the transition of electron from valence band to the local levels to the conduction band as a result of increasing the iron oxide nanoparticles weight percentage[15].

Figure 7 shows the forbidden transition of the indirect energy gap for the (CMC-PVP- Fe_2O_3) nanocomposites.

3.3.5 Refractive Index

Figure 8 shows the change of refraction index for (CMC-PVP- Fe_2O_3) nanocomposites as a function of wavelength, from this figure, it can be noted that the refractive index increases with the increasing of Fe_2O_3 nanoparticles concentration because of an increase in density of nanocomposites. In ultraviolet region, we note high values of the refractive index because of the little transmittance in this region, but in the visible and near IR regions, there are low values because of the high transmittance in this region,

whose behavior is consistent with the researchers N.Abbas *et al.* [10].

3.3.6 Extinction Coefficient

The variation of the extinction coefficient for (CMC-PVP-Fe_2O_3) nanocomposites as a function of wavelength is shown in Figure 9. It can be noted that the extinction coefficient increases with the increase of Fe_2O_3 nanoparticles. This is attributed to the increased absorption coefficient with the increase of weight percentages of Fe_2O_3 nanoparticles . This result indicates that the atoms of (Fe_2O_3) nanoparticles will modify the structure of the host polymer. These results agree with the results of M.A. Habeeb [15]**.**

3.3.7 Real and Imaginary Parts of Dielectric Constant (ε_1,ε_2)

Figure 10 shows the change of (ε_1) as a function of the wavelength. It can be seen that ε_1 considerably depends on (n^2) due to low value of (k^2) so, the real dielectric constant is increased with the increase of the concentrations of (Fe_2O_3) nanoparticles. Figure 11 shows the change of ε_2 as a function of the wavelength. It can be seen that ε_2 is dependent on values that change with the change of the absorption coefficient due to the relation between (α) and (k). These results agree with the results of N. Abbas *et al.* [10].

3.3.8 Optical Conductivity (σ_{op})

Figure 12 shows the variation of optical conductivity as a function of wavelength for (CMC-PVP- Fe_2O_3). The figure shows that the optical conductivity of all samples of nanocomposites are decreased with the increasing of the wavelength. This behavior which attributed to the optical conductivity depends on the wavelength of the radiation incident on the samples of nanocomposites; the increase of optical conductivity at low wavelength of photon is due to high absorbance of all samples of nanocomposites in this region, hence, there is an increase in the charge transfer excitations. The optical conductivity spectra indicated that the samples are transmittance within the visible and near infrared regions . Also, the optical conductivity of nanocomposites is increased with the increase of Fe_2O_3nanoparticles concentrations. This behavior is related to the creation of localized levels in the energy gap; the increase of Fe_2O_3 nanoparticles concentrations leads to increasing the density of localized stages in the band structure, and hence the increase of the absorption coefficient consequently leads to increasing the optical conductivity of (CMC-PVP- Fe_2O_3) [16].

3.2 Application of (CMC-PVP- Fe_2O_3) Nanocomposites for Gamma Ray Shielding

Figures 13 show the variation of (N/N0) for (CMC-PVP) blend with different concentrations of Fe_2O_3 nanoparticles . The transmission radiation decreases with the increasing of the concentrations of Fe_2O_3 nanoparticles which is attributed to the increase of the attenuation radiation [17].

Figure 14 indicate the variety of gamma radiation attenuation coefficients for (CMC- PVP) mix as a function of levels of Fe_2O_3 nanoparticles . The attenuation coefficient increase with increased levels of nanoparticles; this is due to the absorption or reflection of gamma radiation by nanocomposites shielding materials. From the figures, it showed very 0close results by comparing the attained results by polymer nanocomposite with concrete, however, composite polymer has an advantage over concrete because of its mobility, less electrical properties and the ability to avoid neutron emission [18]

4. CONCLUSION

The optical microscope images showed the iron oxide nanoparticles from a continuous network inside the blend at concentration of (0,1.5,3,4.5,6)wt.%. FTIR spectra shows shift in some bands and change in the intensities of other bands comparing with pure (CMC-PVP) films.The absorbance for (CMC-PVP- Fe_2O_3) nanocomposite increases with the increasing of the concentrations of Fe_2O_3 nanoparticles , while the transmittance and the energy gap for (CMC-PVP- Fe_2O_3) nanocomposite decrease with the increasing of the Fe_2O_3 concentrations. The refractive index , extinction coefficient , real and imaginary dielectric constant are increase with increasing of the concentrations of (Fe_2O_3) nanoparticles. The attenuation coefficient increase with increased of concentration.

REFERENCES

1. N.D. Kandpal, Co-precipitation method of synthesis and characterization of iron oxide nanoparticles, Journal of Scientific & Industrial Research.73(2):p.87-90
2. A.M. Abdelghany, E.M. Abdelrazek, D.S. Rashad, Impact of in situ preparation of CdS filled PVP nano-composite. Spectrochim. Acta A Mol. Biomol. Spectrosc. **130**, 302 (2014) https://doi.org/10.1016/j.saa.2014.04.049
3. J. Gurland,"Electrical resistivity", J. Polym. Plast. Technol. Eng. Vol.19, No.1, PP. 21-51, (1982).
4. M. A. Habeeb and L. A. Hamza, " Structural, Optical and D.C Electrical Properties of (PVA-PVP-Y2O3) Films and Their Application for Humidity Sensor", Journal of Advanced Physics, Vol.6, PP.1-9, (2017). https://doi.org/10.1166/jap.2017.1303
5. A.M. Youssef, I.E. El-nagar, A.M.M. El-Torky, A.A. Abd El- Hakim, Development and characterization of CMC/PVA films loaded with ZnO-nanoparticles for antimicrobial packaging application. Der Pharma Chem. **9**(9), 157 (2017).
6. M. Erdem, O. Baykara, M. Dogru, F. Kuluozturk., "A novel shielding material prepared from solid waste containing lead for gamma ray", Phys. and Chem, PP.917-922, (2010). https://doi.org/10.1016/j.radphyschem.2010.04.009

7. M.A. Habeeb, R.S. Abdul Hamza , Novel of (Biopolymer Blend-MgO) Nanocomposites: Fabrication and Characterization for Humidity Sensors ,Journal of Bionanoscience ,12, 328–335 (2018). https://doi.org/10.1166/jbns.2018.1535

8. M.A. Habeeb, R.S. Abdul Hamza,Synthesis of (Polymer blend-MgO) Nanocomposites and Studying Electrical Properties for Piezoelectric Application**,** Indonesian Journal of Electrical Engineering and Informatics, Vol. 6, No. 4, (2018). https://doi.org/10.11591/ijeei.v6i3.511

9. J. Gurland,"Electrical resistivity", J. Polym. Plast. Technol. Eng. Vol.19, No.1, PP. 21-51, (1982).

10. N. K. Abbas,1 M. A.Habeeb,2 A J. Kadham , Preparation of Chloro Penta Amine Cobalt(III)Chloride and Study of Its Influence on the Structural andSome Optical Properties of Polyvinyl Acetate, International Journal of Polymer Science,Vol.15,(2015). https://doi.org/10.1155/2015/926789

11. M.A. Habeeb, A.Hashim, A.Khalaf and A.Hadi, "Fabrication of (PVA-PAA) Blend-Extracts of Plants Bio-Composites and Studying Their Structural, Electrical and Optical Properties for Humidity Sensors Applications", Sensor Letters, Vol.15, No.7, doi:10.1166/sl.2017.3856, (2017). https://doi.org/10.1166/sl.2017.3856

12. M. Dahshan,"Introduction to Material Science and engineering", 2nd, McGraw Hill, New york, (2002).

13. M. Crane, "Solar Cells", translation Y. Hassan, Collage of Education, University of Mousl, (1989).

14. A. Hashim, M.A.Habeeb, Synthesis and Characterization of Polymer Blend-$CoFe_2O_4$ Nanoparticles as a Humidity Sensors for Different Temperatures , Transactions on Electrical and Electronic Materials, Vol.20,Issue2, pp.107-112, DOI: 10.1007/s42341-018-0081-1, (2019). https://doi.org/10.1007/s42341-018-0081-1

15. M.A. Habeeb, Effect of rat of deposition on the optical parameters of GaAs films ,Euro Journal of Scientific Research ,Vol.57, No.3, (2011).

16. M.A. Habeeb, Dielectric and Optical Properties of (PVAc-PEG-Ber) Biocomposites, Journal of Engineering and Applied Sciences, Vol.9,No.4,(2014).

17. A. Hashim, M. A. Habeeb, Structural and Optical Properties of (Biopolymer Blend-Metal Oxide) Bionanocomposites for Humidity Sensors, Journal of Bionanoscience, Vol.12, No.5, doi:10.1166/jbns.2018.1578 , (2018). https://doi.org/10.1166/jbns.2018.1578

18. M. A. Habeeb, A Hashim, and A. Hadi,"Fabrication of New Nanocomposites:- CMC-PAA-PbO2Nanoparticles for Piezoelectric Sensors and Gamma Radiation Shielding Applications ", Vol.15, doi:10.1166/sl.2017.3877, (2017). https://doi.org/10.1166/sl.2017.3877

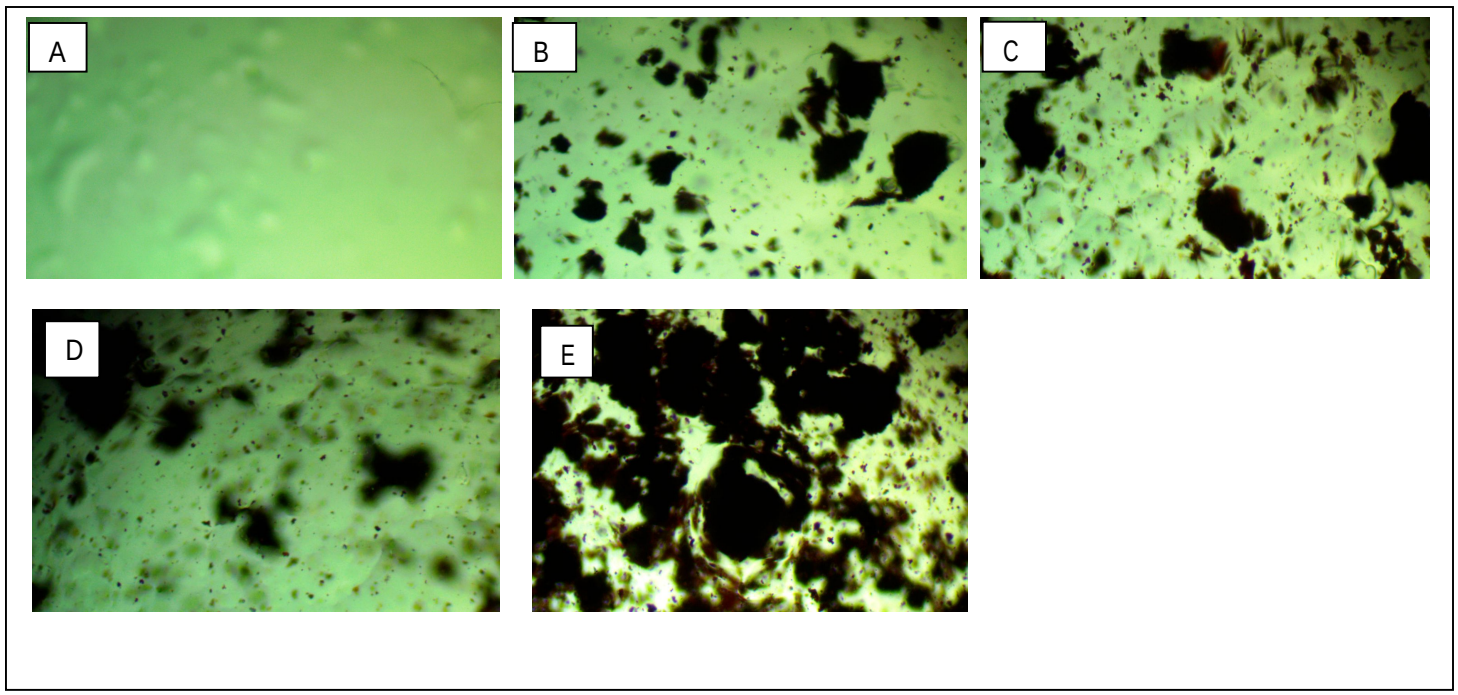

Figure 1: Photomicrographs (10X) for (CMC-PVP-Fe_2O_3) nanocomposites:(A)(pure),(B) 1.5 wt.%Fe_2O_3,(C)3wt.%Fe_2O_3 ,(D) 4.5 wt.% Fe_2O_3 ,(E) 6 wt.%Fe_2O_3.

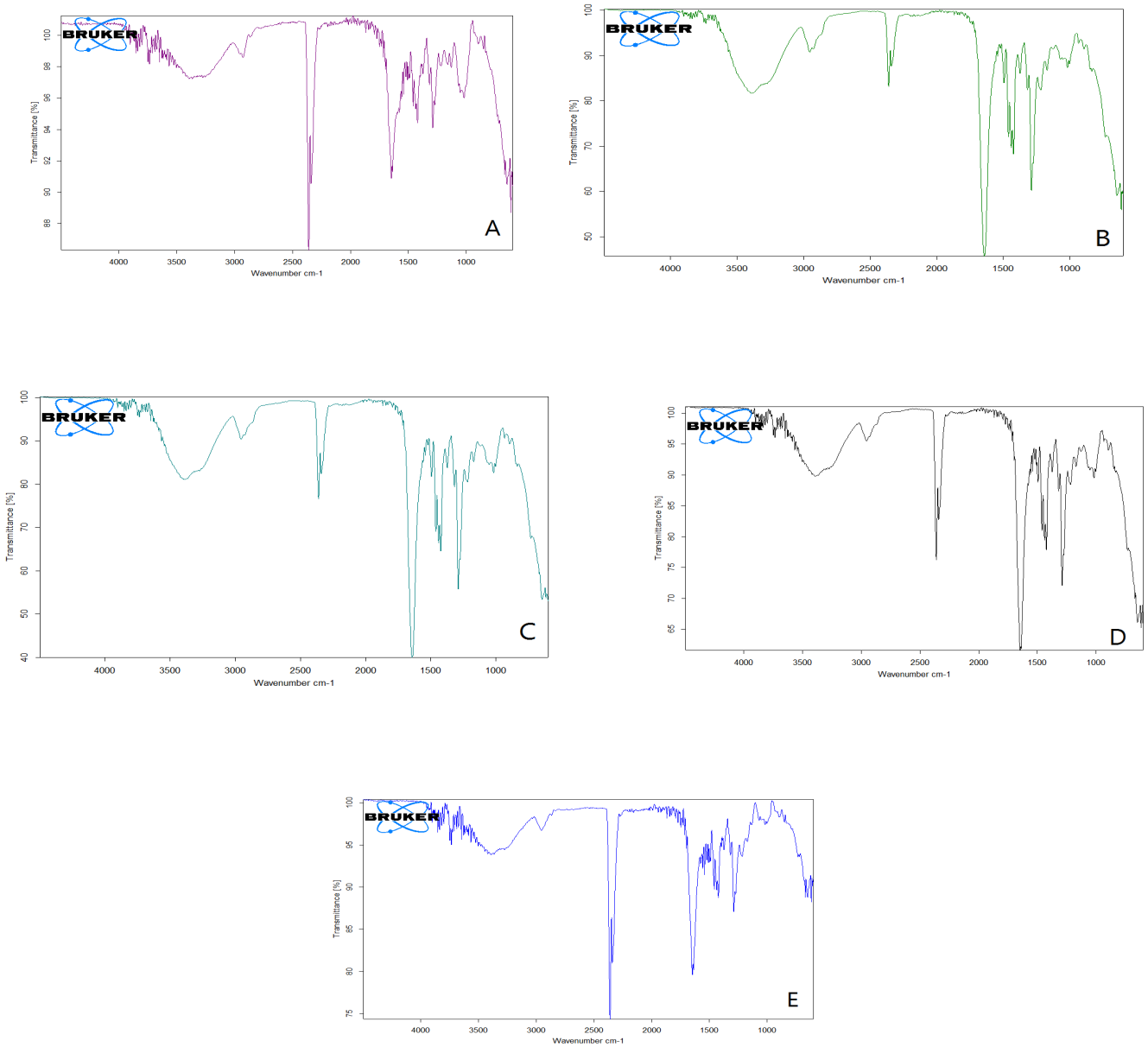

Figure 2: FTIR spectra for (CMC-PVP-Fe_2O_3) nanocomposites films, (A) pure(CMC- PVP) film,(B)1.5wt.% Fe_2O_3,(C) 3wt.% Fe_2O_3 ,(D) 4.5 wt.% Fe_2O_3 , (E) 6wt.%Fe_2O_3.

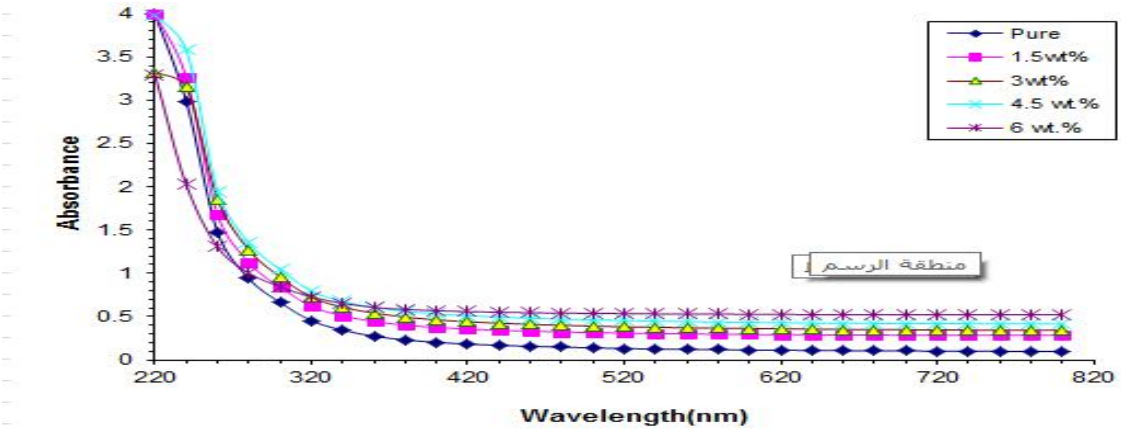

Figure 3: Absorbance spectra with photon wavelength of (CMC-PVP-Fe_2O_3) nanocomposites.

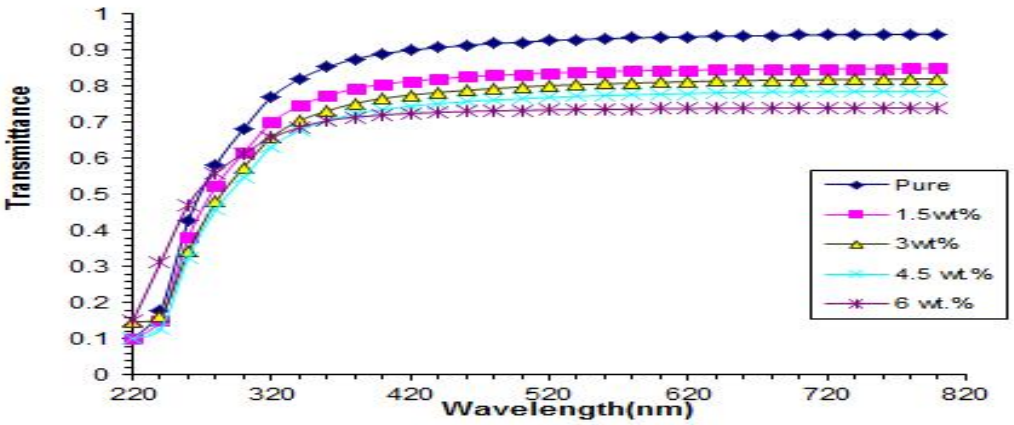

Figure 4: Transmittance spectra of (CMC-PVP- Fe_2O_3) nanocomposites as a function of wavelength.

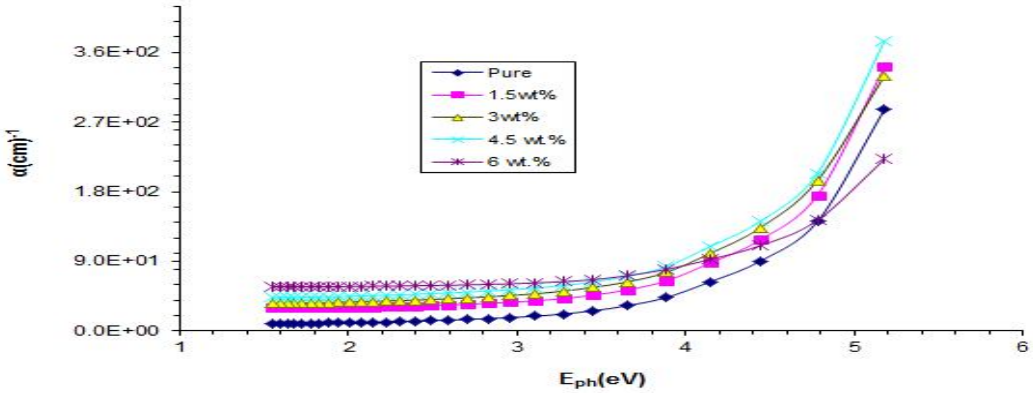

.

Figure 5: Variation of absorption coefficient for (CMC-PVP- Fe_2O_3) nanocomposites with photon energy.

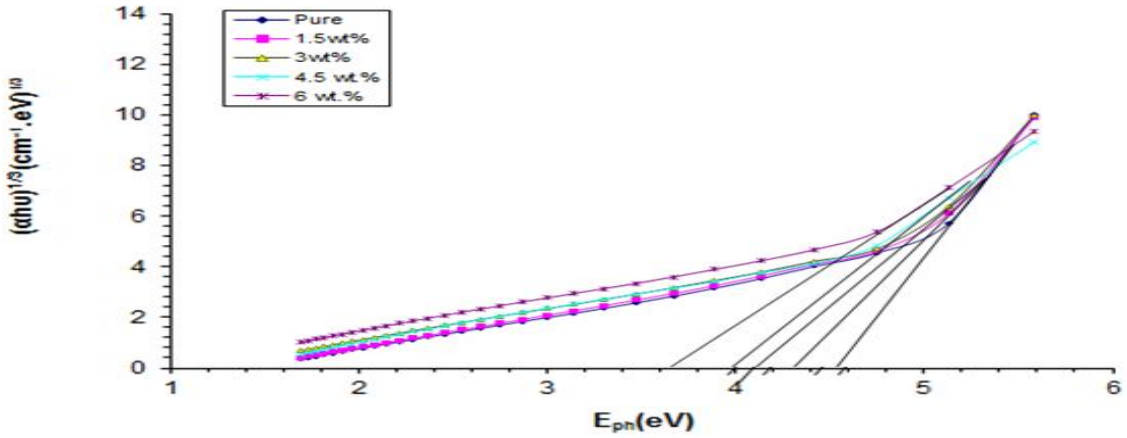

Figure 6: The relationship between $(\alpha h\upsilon)^{1/2}(cm^{-1}.eV)^{1/2}$and photon energy of (CMC-PVP-Fe_2O_3) nanocomposites.

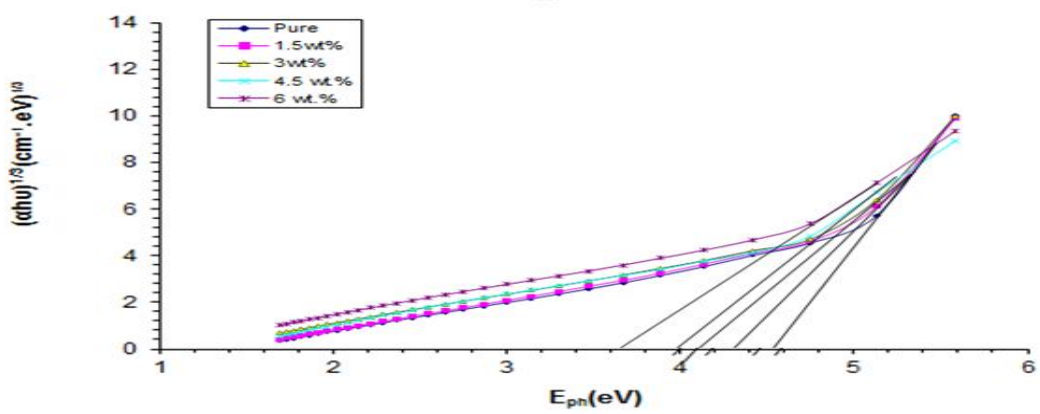

Figure 7: The relationship between $(\alpha h\upsilon)^{1/3}(cm^{-1}.eV)^{1/3}$and photon energy of (CMC-PVP- Fe_2O_3) nanocomposites.

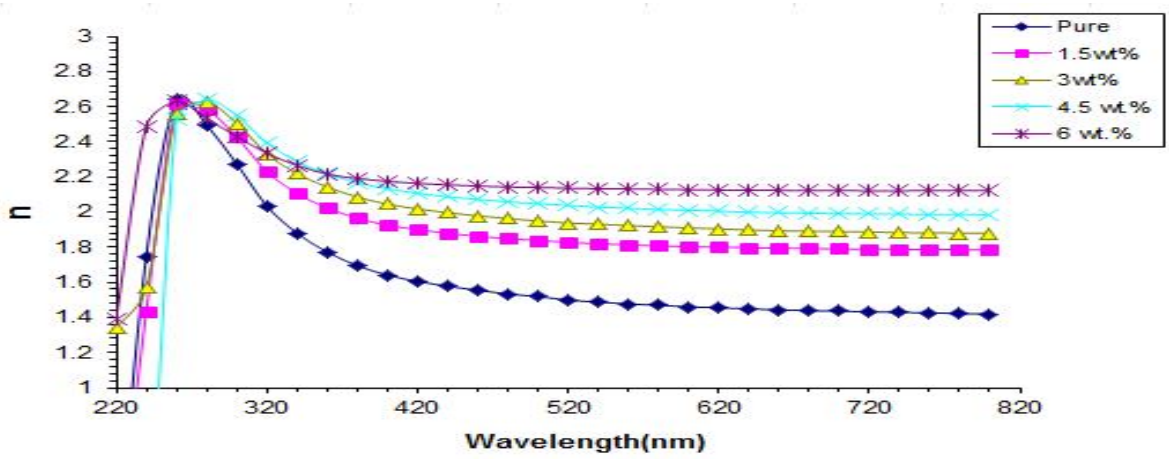

Figure 8: The refractive index as a function of wavelength for (CMC-PVP- Fe_2O_3) nanocomposites.

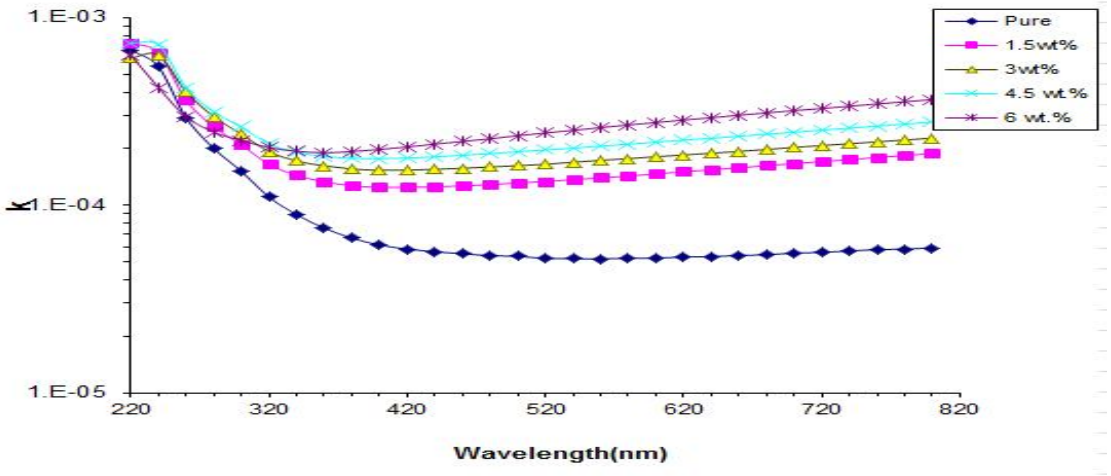

Figure 9: Variation of extinction coefficient of (CMC-PVP- Fe_2O_3) nanocomposites with wavelength**.**

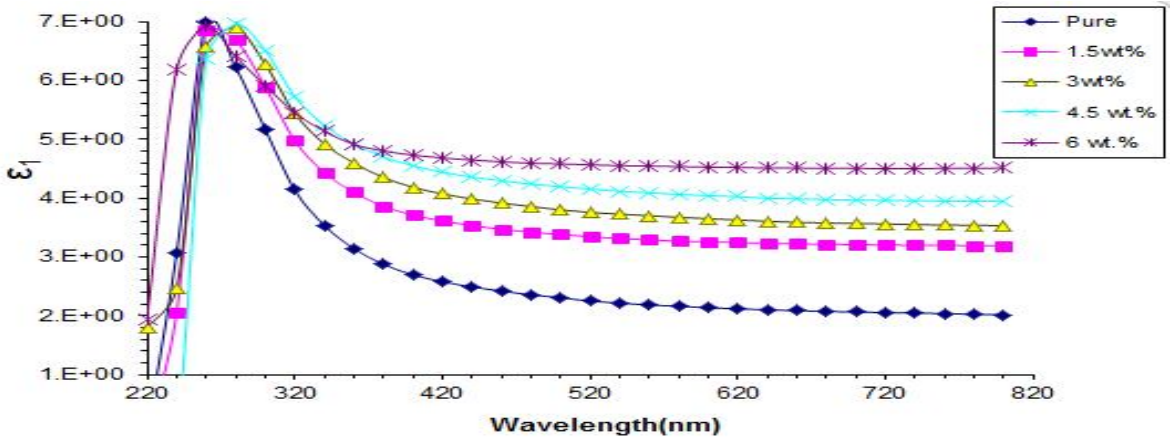

Figure 10: The real dielectric constant as a function of incident wavelength for (CMC-PVP- Fe_2O_3) nanocomposites.

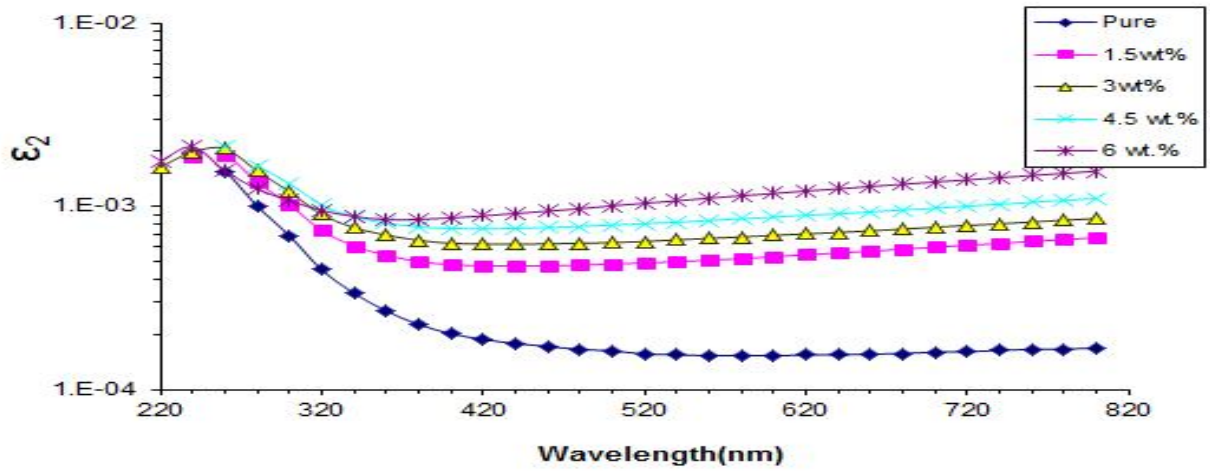

Figure 1): The imaginary dielectric constant as a function of wavelength for (CMC-PVP- Fe_2O_3) nanocomposites.

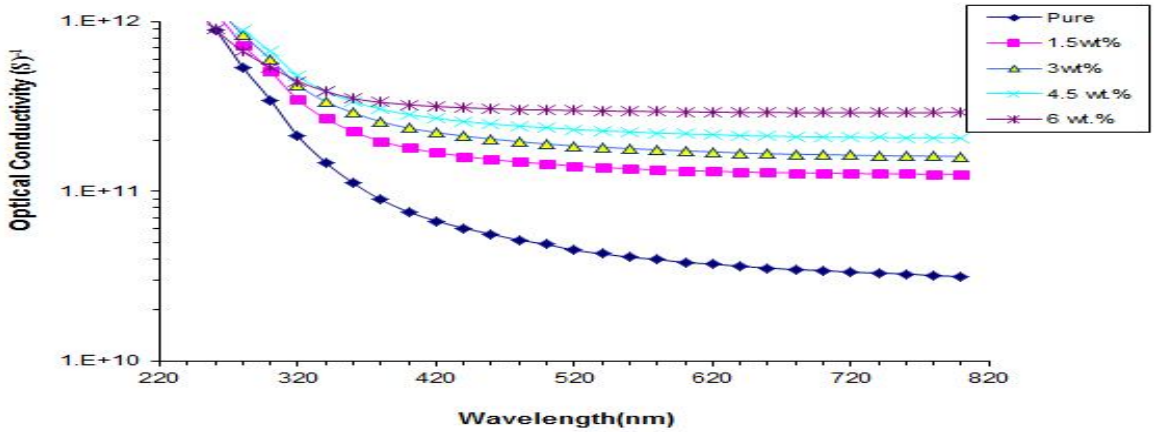

Figure 12: Optical conductivity of (CMC-PVP- Fe_2O_3) nanocomposites as afunction of wavelength.

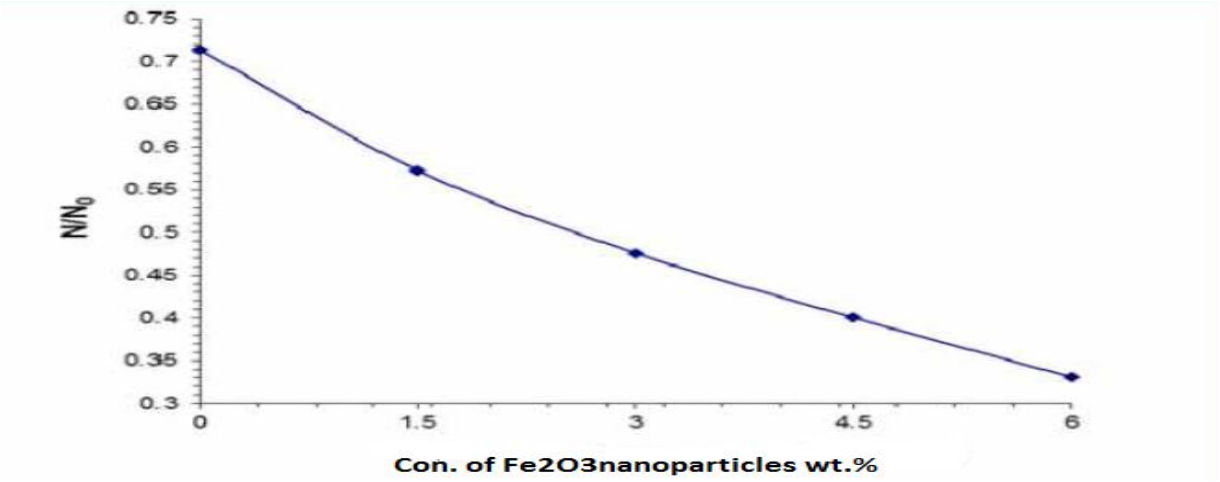

Figure 13: Variation of (N/N0) for (CMC- PVP) blend with different concentrations of Fe_2O_3 nanoparticles.

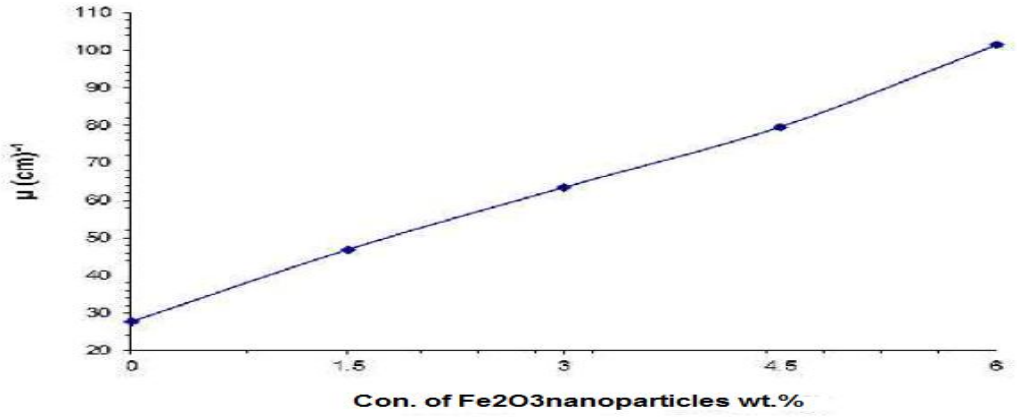

.

Figure 14: Variation of attenuation coefficient of gamma radiation for (CMC-PVP) blend as a function of Fe_2O_3 nanoparticles concentrations.